Inorganic Chemistry
Article

Inorg. Chem. **2010**, *49*, 9609–9616 **9609**
DOI: 10.1021/ic101357y

The Use of Polarizable $[AuX_2(CN)_2]^-$ (X = Br, I) Building Blocks Toward the Formation of Birefringent Coordination Polymers

Jeffrey S. Ovens, Andrew R. Geisheimer, Alexei A. Bokov, Zuo-Guang Ye,* and Daniel B. Leznoff*

Department of Chemistry, Simon Fraser University, 8888 University Drive, Burnaby, British Columbia, V5A 1S6, Canada

Received July 7, 2010

The $[^nBu_4N][AuX_2(CN)_2]$ (X = Br, I) salts were synthesized and structurally characterized. Both feature square-planar $[AuX_2(CN)_2]^-$ anions, with trans cyano and halo ligands, which aggregate via halogen−halogen interactions. The aggregation of $[AuX_2(CN)_2]^-$ units results in the parallel alignment of all of the Br−Au−Br moieties in the anions along the [110] and [1$\bar{1}$0] directions. Two crystal habits of $[^nBu_4N][AuBr_2(CN)_2]$ were grown: with (1$\bar{1}$0) and (001) as the primary faces. The birefringence in the (1$\bar{1}$0) plane was found to be $\Delta n = 0.051(4)$ and was <0.03 in the (001) plane. Using the $[AuBr_2(CN)_2]^-$ unit, $[M(phen)_2][AuBr_2(CN)_2]_2$ (M = Fe, Ni), $[Ni(terpy)_2][AuBr_2(CN)_2]_2$, $[Fe(terpy)_2][AuBr_2(CN)_2][ClO_4]$, and $[Cu(phen)_2(NO_3)][AuBr_2(CN)_2]$ (phen = 1,10-phenanthroline, terpy = 2,2′;6′,2″-terpyridine) were synthesized and structurally characterized: they formed ionic structures with coordinatively saturated metal cations and structurally aligning Br···Br interactions between the $[AuBr_2(CN)_2]^-$ anions. A molecular complex, $Cu(terpy)[AuBr_2(CN)_2]_2$, was prepared, as well as the coordination polymer, $[Ni(en)_2(AuBr_2(CN)_2)][AuBr_2(CN)_2]\cdot MeOH$ (en = ethylenediamine). The structure consists of layers of chains of $Ni(en)_2(AuBr_2(CN)_2)^+$ units and chains of unbound $[AuBr_2(CN)_2]^-$ units formed via Br···Br interactions; a $\Delta n = 0.131(3)$ was measured. The Δn values were related to the supramolecular structures in terms of the relative intermolecular alignment of Br−Au−Br and NC−Au−CN bonds. These measurements both demonstrate the utility of the Au−Br bonds in enhancing birefringence and show that the contribution of the M−CN units to the overall birefringence of cyanometallate coordinations polymers is non-negligible.

Introduction

The nearly limitless design possibilities inherent in coordination polymer research have resulted in intense interest in these materials.[1−3] This feature of coordination polymers—the ability to strategically design their supramolecular structure using a judicious choice of modular building blocks[4−7]—has been harnessed to manifest or enhance useful properties such as magnetism,[8−11] conductivity,[12−15] or porosity.[16−18]

Recently, it has been shown that coordination polymers can be designed to provide a structural framework invaluable to the enhancement of birefringence (the difference in refractive index of a material depending on crystallographic direction).[19−21] Birefringent materials have a wide range of applications, including in optical filters,[22,23] waveplates,[24]

*To whom correspondence should be addressed. E-mail: zye@sfu.ca (Z.-G.Y.); dleznoff@sfu.ca. (D.B.L.).

(1) Janiak, C. *Dalton Trans.* **2003**, 2781.
(2) Batten, S. R.; Robson, R. *Angew. Chem. Int. Ed.* **1998**, *37*, 1460.
(3) Moulton, B.; Zaworotko, M. J. *Chem. Rev.* **2001**, *101*, 1629.
(4) James, S. L. *Chem. Soc. Rev.* **2003**, *32*, 276.
(5) Kitagawa, S.; Kitaura, R.; Noro, S.-i. *Angew. Chem., Int. Ed.* **2004**, *43*, 2334.
(6) Decurtins, S.; Pellaux, R.; Antorrena, G.; Palacio, F. *Coord. Chem. Rev.* **1999**, *190−192*, 841.
(7) Madalan, A. M.; Avarvari, N.; Andruh, M. *Cryst. Growth Des.* **2006**, *6*, 1671.
(8) Lefebvre, J.; Chartrand, D.; Leznoff, D. B. *Polyhedron* **2007**, *26*, 2189.
(9) Lefebvre, J.; Tyagi, P.; Trudel, S.; Pacradouni, V.; Kaiser, C.; Sonier, J. E.; Leznoff, D. B. *Inorg. Chem.* **2009**, *48*, 55.
(10) Ruiz, E.; Rodríguez-Fortea, A.; Alvarez, S.; Verdaguer, M. *Chem.—Eur. J.* **2005**, *11*, 2135–44.
(11) Tey, S. L.; Reddy, M. V.; Subba Rao, G. V.; Chowdari, B. V. R.; Yi, J.; Ding, J.; Vittal, J. J. *Chem. Mater.* **2006**, *18*, 1587.
(12) Welte, L.; Calzolari, A.; Di Felice, R.; Zamora, F.; Gómez-Herrero, J. *Nat. Nanotechnol.* **2010**, *5*, 110.
(13) Takaishi, S.; Hosoda, M.; Kajiwara, T.; Miyasaka, H.; Yamashita, M.; Nakanishi, Y.; Kitagawa, Y.; Yamaguchi, K.; Kobayashi, A.; Kitagawa, H. *Inorg. Chem.* **2009**, *48*, 9048.
(14) Delgado, S.; Sanz Miguel, P. J.; Priego, J. L.; Jiménez-Aparicio, R.; Gómez-García, C. J.; Zamora, F. *Inorg. Chem.* **2008**, *47*, 9128.
(15) Hurd, J. A.; Vaidhyanathan, R.; Thangadurai, V.; Ratcliffe, C. I.; Moudrakovski, I. L.; Shimizu, G. K. H. *Nat. Chem.* **2009**, *1*, 705.
(16) Rosi, N. L.; Eddaoudi, M.; Kim, J.; O'Keeffe, M.; Yaghi, O. M. *CrystEngComm* **2002**, *4*, 401.
(17) Rowsell, J. L. C.; Yaghi, O. M. *Angew. Chem., Int. Ed.* **2005**, *44*, 4670.
(18) Dincă, M.; Dailly, A.; Liu, Y.; Brown, C. M.; Neumann, D. A.; Long, J. R. *J. Am. Chem. Soc.* **2006**, *128*, 16876.
(19) Katz, M. J.; Kaluarachchi, H.; Batchelor, R. J.; Bokov, A. A.; Ye, Z.-G.; Leznoff, D. B. *Angew. Chem., Int. Ed.* **2007**, *46*, 8804.
(20) Katz, M. J.; Leznoff, D. B. *J. Am. Chem. Soc.* **2009**, *131*, 18435.
(21) Draper, N. D.; Batchelor, R. J.; Sih, B. C.; Ye, Z.-G.; Leznoff, D. B. *Chem. Mater.* **2003**, *15*, 1612.
(22) Velasquez, P.; del Mar Sánchez-López, M.; Moreno, I.; Puerto, D.; Mateos, F. *Am. J. Phys.* **2005**, *73*, 357.
(23) Saeed, S.; Bos, P. J.; Li, Z. *Jpn. J. Appl. Phys., Part 1* **2001**, *40*, 3266.
(24) Lipson, S. G.; H, L.; Tannhauser, D. S. *Optical Physics*, 3rd ed.; Cambridge University Press: Cambridge, U. K., 1995.

Published on Web 09/22/2010

liquid-crystal displays,[25−27] and nonlinear optical processes.[28−30]

In order for a material to be birefringent, the overall electronic polarizability, which is dependent on both the polarizabilities of the individual molecular components as well as local electric fields, must be anisotropic.[31−33] This may be achieved by aligning, in a parallel fashion, highly polarizable bonds in the crystal in order to enhance their individual polarizabilities; an anisotropic structural motif is also invaluable. With these principles in mind, we previously utilized the anisotropic $[Au(CN)_2]^-$ building block to prepare heterobimetallic Pb/$[Au(CN)_2]^-$-based coordination polymer frameworks, which enforced the alignment of polarizable, anisotropic 2,2′;6′,2″-terpyridine (terpy) ligands as a means to enhance birefringence (Δn).[19,34] These materials had Δn values of 0.39−0.43, which are greater than double the 0.17 value found for calcite, the commercial standard.[31−33,35] The inclusion of highly polarizable C−X (X = Cl, Br) bonds to the 4′-position of terpy yielded coordination polymers with Δn ranging from 0.26−0.50 depending on the orientation of the C−X bond relative to the optical axis.[20] This result clearly showed that the strategically placed addition of polarizable bonds could significantly impact the observed birefringence values.

Instead of functionalizing the ligand, we consider in this contribution adding polarizable bonds to the cyanometallate unit. For this purpose, the neglected $[AuX_2(CN)_2]^-$ (X = Br, I) system was targeted. This d^8 gold(III) building block is rendered effectively linear (comparable geometrically to $[Au(CN)_2]^-$), since only through the trans cyanide ligands will metal cations bind. More importantly, the highly polarizable Au−X bonds[36] may be able to promote an enhancement of birefringence, as was the case for some halo-substituted terpy-containing materials.[20] A critical requirement vis a vis toward using the $[AuX_2(CN)_2]^-$ units as birefringence-enhancing units is that their supramolecular alignment must be "favorable". For example, alignment of the $[Au(CN)_2]^-$ units in related cyanoaurate(I) coordination polymers is enhanced by the formation of attractive aurophilic interactions.[19,37,38] However, analogous d^8−d^8 Au(III) interactions are rare[37] and have never been observed in the few examples of related $[Au(CN)_4]^-$-containing coordination polymers.[39−43] On the other hand, weak halogen−halogen interactions[44−46] could play a similar role as aurophilicity in impacting the supramolecular structures of $[AuX_2(CN)_2]^-$-containing coordination polymers.

As a first step toward utilizing $[AuX_2(CN)_2]^-$ units to influence birefringence, since no coordination polymers have been reported using the $[AuX_2(CN)_2]^-$ system, it is necessary to assess both the ability of this unit as a building block in forming new coordination polymers in general and, more importantly, its propensity to increase the structural alignment (and ultimately the birefringence) of materials. Thus, herein, the synthesis and characterization of $[AuX_2(CN)_2]^-$ (X = Br, I) units and the structural and superstructural behavior of the bromo analogue when combined with first row transition metal complex cations as well as a structure-birefringence analysis of some of the materials are described.

Results and Discussion

Synthesis and Structures of the $[AuX_2(CN)_2]^-$ Building Blocks. The addition of neat Br_2 to an aqueous solution of $K[Au(CN)_2]$ yielded a yellow solution of $K[AuBr_2(CN)_2]$ via oxidative addition of the Br_2 to the Au(I) center.[47] Cation exchange of K^+ with $^nBu_4N^+$ via the addition of $[^nBu_4N]Br$ resulted in the yellow solid $[^nBu_4N][AuBr_2(CN)_2]$ (**1**). In the IR spectrum, the ν_{CN} band shifted accordingly from 2141 to 2167 cm^{-1}, accompanied by a significant weakening of intensity as observed for the related $[Au(CN)_4]^-$-based systems.[42,43,48] No crystal structure of the $[AuX_2(CN)_2]^-$ series of cyanoaurate(III) building blocks has been previously reported, and thus single crystals of **1** were grown for that purpose by slow evaporation of a MeOH solution.

The X-ray structure reveals the expected square-planar Au(III) center with trans-Br and -CN ligands. The Au−C and Au−Br bond lengths of 2.003(6) and 2.4120(5) Å, respectively, are unremarkable and comparable to other such distances.[41,42,49] Of greater interest is the intermolecular packing of the $[AuBr_2(CN)_2]^-$ units. Rather than crystallizing as well-separated ion pairs, or forming M···M interactions typical for Au(I) and Pt(II),[37] or forming Au−CN···Au interactions as observed for $[Au(CN)_4]^-$,[40] the anions form 1-D chains along the [110] and [1$\bar{1}$0] directions by virtue of Br···Br interactions.[44,45] The latter direction also corresponds to the principal plane of crystal growth when grown via slow evaporation of a MeOH solution. The distance is 3.5156(11) Å, which is smaller than the sum of the van der Waals radii of

(25) Wu, S.-T.; Wu, C.-S. *Appl. Phys. Lett*. **1996**, *68*, 1455.
(26) Schadt, M. *Jpn. J. Appl. Phys* **2009**, *48*, 03B001.
(27) Ong, H. L. *Appl. Phys. Lett*. **1991**, *59*, 155.
(28) Bosshard, C. *Adv. Mater*. **1996**, *8*, 385.
(29) Golovan, L. A.; Timoshenko, V. Y.; Fedotov, A. B.; Kuznetsova, L. P.; Sidorov-Biryukov, D. A.; Kashkarov, P. K.; Zheltikov, A. M.; Kovalev, D.; Künzner, N.; Gross, E.; Diener, J.; Polisski, G.; Kock, F. *Appl. Phys. B: Lasers Opt*. **2001**, *73*, 31.
(30) Fiore, A.; Berger, V.; Rosencher, E.; Bravetti, P.; Nagle, J. *Nature* **1998**, *391*, 463.
(31) Hecht, E. *Optics*, 4th ed.; Addison Wesley: San Francisco, 2002.
(32) Newnham, R. E. *Structure−Property Relations*; Springer-Verlag: New York, 1975.
(33) Newnham, R. E. *Properties of Materials: Anisotropy, Symmetry, Structure*; Oxford University Press: New York, 2005.
(34) Katz, M. J.; Aguiar, P. M.; Batchelor, R. J.; Bokov, A. A.; Ye, Z.-G.; Kroeker, S.; Leznoff, D. B. *J. Am. Chem. Soc*. **2006**, *128*, 3669.
(35) Weber, M. J. *Handbook of Optical Materials*; CRC Press: Boca Raton, FL, 2003.
(36) *CRC Handbook of Chemistry and Physics*, 71st ed.; Lide, D. R., Ed.; CRC Press, Inc.: Boca Raton, FL, 1990.
(37) Katz, M. J.; Sakai, K.; Leznoff, D. B. *Chem. Soc. Rev*. **2008**, *37*, 1884.
(38) Mohamed, A. A.; Abdou, H. E.; Fackler, J. P. *Inorg. Chem*. **2006**, *45*, 11.
(39) Katz, M. J.; Shorrock, C. J.; Batchelor, R. J.; Leznoff, D. B. *Inorg. Chem*. **2006**, *45*, 1757.
(40) Katz, M. J.; Kaluarachchi, H.; Batchelor, R. J.; Schatte, G.; Leznoff, D. B. *Cryst. Growth Des*. **2007**, *7*, 1946.
(41) Leznoff, D. B.; Shorrock, C. J.; Batchelor, R. J. *Gold Bull*. **2007**, *40*, 36.
(42) Shorrock, C. J.; Jong, H.; Batchelor, R. J.; Leznoff, D. B. *Inorg. Chem*. **2003**, *42*, 3917.
(43) Vitoria, P.; Muga, I.; Gutiérrez-Zorilla, J. M.; Luque, A.; Román, P.; Lezama, L.; Zúniga, F. J.; Beitia, J. I. *Inorg. Chem*. **2003**, *42*, 960.
(44) Navon, O.; Bernstein, J.; Khodorkovsky, V. *Angew. Chem., Int. Ed*. **1997**, *36*, 601.
(45) Desiraju, G. R.; Parthasarathy, R. *J. Am. Chem. Soc*. **1989**, *111*, 8725.
(46) *Halogen Bonding: Fundamentals and Applications*; Mingos, D. M. P., Ed.; Springer-Verlag: Berlin, 2008.
(47) Mason, W. R. *Inorg. Chem*. **1970**, *9*, 2688.
(48) Jones, L. H.; Smith, M. J. *J. Chem. Phys*. **1964**, *41*, 2507.
(49) Baidina, I. A.; Makotchenko, E. V. *J. Struct. Chem*. **2010**, *51*, 187.

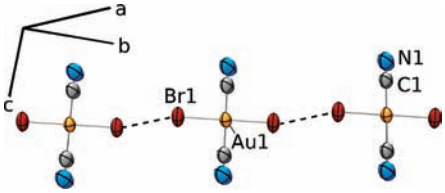

Figure 1. 1-D anionic chains of **1** (^{n}Bu$_4$N$^+$ cations removed for clarity). Br···Br interactions are shown as dashed lines. Au, yellow; Br, scarlet; C, gray; N, blue.

two Br atoms (3.70 Å),[50] indicating that a viable halogen−halogen interaction exists. As shown in Figure 1, the $[AuBr_2(CN)_2]^-$ anions orient themselves such that the bromide ligands form a stepwise chain; this also results in the parallel alignment of $[AuBr_2(CN)_2]^-$ moieties along the [110] and [1$\bar{1}$0] directions. The Au−Br···Br angle between units is 150.77(3)°.

Analogously, the addition of a CH_2Cl_2 solution of I_2 to a CH_2Cl_2 solution of $[^nBu_4N][Au(CN)_2]\cdot 1/2H_2O$ yielded an orange solution of $[^nBu_4N][AuI_2(CN)_2]$ (**2**) via oxidative addition of I_2 to the Au(I) center. In the IR spectrum of the isolated solid, the ν_{CN} band shifted from 2141 to 2165 cm^{-1}. Single crystals of **2** were grown by slow evaporation of a methanol solution.

As with **1**, the X-ray structure of **2** shows a square-planar geometry about the Au center with *trans*-I and -CN ligands, with typical Au−C and Au−I bond lengths of 2.002(16) and 2.6064(14) Å, respectively. Similar to **1**, the $[AuI_2(CN)_2]^-$ anions aggregate intermolecularly to form 1-D chains. In contrast to the stepwise pattern seen in **1**, the anions form a zigzag motif (Figure 2), orienting themselves with a Au−I···I angle of 96.23(4)°. The interactions have a length of 3.7879(17) Å, which is smaller than the sum of the van der Waals radii of two I atoms (3.96 Å).[50]

Halogen−halogen interactions have been widely recognized, particularly in halogenated organic molecules in the solid state,[45] with interaction distances of 3.4−3.7 Å for Br···Br[44] and up to 4.0 Å for I···I,[45] and reported bond stabilization energies up to $E_s = 8.12$ kJ mol (varying as $Cl^- < Br^- < I^-$).[44,51] These are substantially weaker than typical hydrogen bonds[52] but are nevertheless sufficient to induce a significant degree of preferential alignment of molecules in the solid state. *Ab initio* studies probing the orientation of these interactions have shown both stepwise and zigzag geometries to be preferred.[51] The presence of these interactions and the knowledge of their behavior may assist in increasing structural dimensionality in coordination polymers that incorporate appropriate halogenated building blocks such as $[AuX_2(CN_2)]^-$.

Structures of $[AuBr_2(CN_2)]^-$ Salts with Coordinatively Saturated Cations. We targeted the synthesis of coordination polymers with the $[AuBr_2(CN)_2]^-$ building block which also incorporated ligands likely to promote high birefringence, i.e., polarizable, flat heterocyclic donors such as 1,10-phenanthroline (phen) and terpy; for example, the prototypical Pb(terpy)$[Au(CN)_2]_2$ system showed

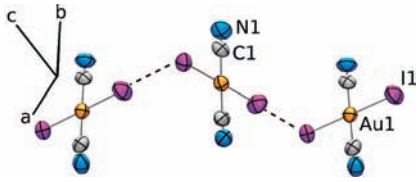

Figure 2. 1-D anionic chains of **2** (^{n}Bu$_4$N$^+$ cations removed for clarity). I···I interactions are shown as dashed lines. Au, yellow; I, purple; C, gray; N, blue.

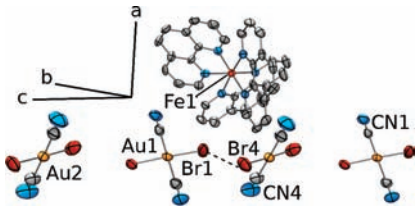

Figure 3. Crystal structure of **3** (hydrogen atoms removed for clarity). The Br1···Br4 interaction is shown. CN1 represents the group containing atoms C1 and N1. Au, yellow; Br, scarlet; Fe, orange; C, gray; N, blue.

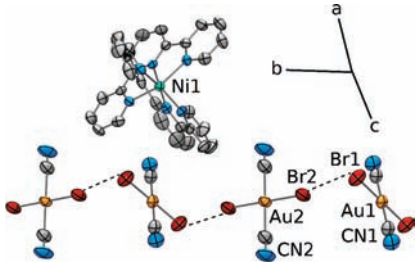

Figure 4. Crystal structure of **5** (hydrogen atoms removed for clarity). The Br1···Br2 interactions are shown. CN1 represents the group containing atoms C1 and N1. Au, yellow; Br, scarlet; Ni, aqua; C, gray; N, blue.

$\Delta n = 0.396(8)$.[19] However, in many cases, despite the substoichiometric addition of ligand, a coordinatively saturated metal−cation was generated, leaving unbound $[AuBr_2(CN)_2]^-$, which aggregated via Br···Br interactions in some cases. For example, when MeOH solutions of $[Fe(ClO)_4]_2\cdot xH_2O$, 2 equivalents of phen, and $[^nBu_4N][AuBr_2(CN)_2]$ were mixed, the salt $[Fe(phen)_3][AuBr_2(CN)_2]_2$ (**3**) was formed, consisting of an ionic network of $[Fe(phen)_3]^{2+}$ cations and $[AuBr_2(CN)_2]^-$ anions (Figure 3). The $[AuBr_2(CN)_2]^-$ anions are arranged in a chain such as is seen in **1**; however, the chain in **3** is segmented, as only every other distance (3.612(2) Å) is less than the sum of the van der Waals radii. The other pairs have an internuclear distance of 4.0658(19) Å. The Au−Br···Br angle between the connected pairs of anions is 146.96(8)°.

A similar packing motif is seen when Ni(II) is used instead of Fe(II), generating the isostructural $[Ni(phen)_3][AuBr_2(CN)_2]_2$ (**4**), and also is seen in $[Ni(terpy)_2][AuBr_2(CN)_2]_2$ (**5**), which is formed from the addition of 1 equivalent of terpy instead of phen. Compounds **4** and **5** both contain coordinatively saturated octahedral metal−cations. Compound **4** contains the broken chains of $[AuBr_2(CN)_2]^-$ units seen in **3**, with intermolecular Br1···Br4 distances of 3.631(3) and 4.266(2) Å, and a Au−Br···Br angle of 147.53(9), while **5** (Figure 4) contains the zigzag motif seen in **2** with an intermolecular Br1···Br2 distance of 3.6208(17) Å, with a Au−Br···Br angle of 88.31(4).

(50) Bondi, A. *J. Phys. Chem.* **1964**, *68*, 441.
(51) Awwadi, F. F.; Willett, R. D.; Peterson, K. A.; Twamley, B. *Chem.—Eur. J.* **2006**, *12*, 8952.
(52) Jeffrey, G. A. *An Introduction to Hydrogen Bonding* (*Topics in Physical Chemistry*); Oxford University Press: Oxford, U. K., 1997.

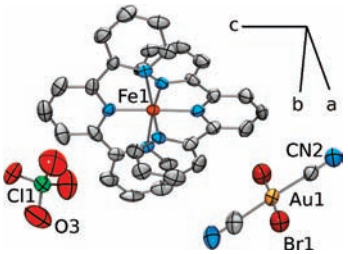

Figure 5. Ionic structure of **6** (hydrogen atoms removed for clarity). CN2 represents the group containing atoms C2 and N2. Au, yellow; Br, scarlet; Cl, green; Fe, orange; O, red; C, gray; N, blue.

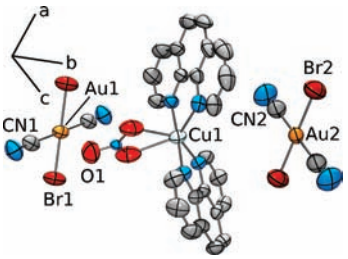

Figure 6. Crystal structure of **7** (hydrogen atoms removed for clarity). CN1 represents the group containing atoms C1 and N1. Au, yellow; Br, scarlet; Cu, l. blue; O, red; C, gray; N, blue.

Clearly, the differences in energy minima between these two supramolecular arrangements is quite small.

In some cases, anions from the M(II) salt precursor were incorporated into the structure, either bound to the metal cation or as a free anion. To maintain charge balance, the stoichiometry of the $[AuBr_2(CN)_2]^-$ unit decreased. For example, when $Fe(ClO_4)_2 \cdot xH_2O$, 1 equivalent of terpy, and $[^nBu_4N][AuBr_2(CN)_2]$ were mixed, $[Fe(terpy)_2][ClO_4]$-$[AuBr_2(CN)_2]$ (**6**; Figure 5) was formed, containing one unbound ClO_4^- and one $[AuBr_2(CN)_2]^-$ unit; no anion aggregation occurs in this case.

When MeOH solutions of $Cu(NO_3)_2 \cdot 6H_2O$, phen, and $[^nBu_4N][AuBr_2(CN)_2]$ were mixed, $[Cu(NO_3)(phen)_2]$-$[AuBr_2(CN)_2]$ (**7**) was formed, in which a bidentate nitrate ligand is bound to the Cu(II) center (Figure 6); again, no anion aggregation occurs in this case.

Characteristic of the unbound $[AuBr_2(CN)_2]^-$ units in **3**−**7** are the ν_{CN} values, which are practically unshifted at approximately 2168 cm^{-1} (c.f., 2167 cm^{-1} for the building block salt).

Structures of Coordination Complexes and Polymers with Bound $[AuBr_2(CN)_2]^-$. In contrast to Ni(II) and Fe(II), the addition of $Cu(ClO_4)_2 \cdot 6H_2O$, 1 equivalent of terpy, and 2 equivalents of $[^nBu_4N][AuBr_2(CN)_2]$ yielded green crystals of $Cu(terpy)[AuBr_2(CN)_2]_2$ (**8**), which features a molecular system containing a five-coordinate Cu(II) center bound by terpy and two $[AuBr_2(CN)_2]^-$ units ligated through the N-cyano donors. The Cu−NC−Au binding is observed in the IR, with blue-shifted ν_{CN} peaks at 2222, 2206, and 2177 cm^{-1}.[53] The breaking of symmetry in the $[AuBr_2(CN)_2]^-$ units also produces multiple peaks.

The geometry of the Cu(II) center in **8** is best described as square-pyramidal, with the terpy and one $[AuBr_2(CN)_2]^-$ unit forming the base and the remaining $[AuBr_2(CN)_2]^-$ unit forming the apex, as shown in Figure 7. The base is not perfectly square due to the geometry constraints imposed by the chelating terpy ligand (Table 1).

(53) Dunbar, K. R.; Heintz, R. A. *Prog. Inorg. Chem.* **1997**, *45*, 283.

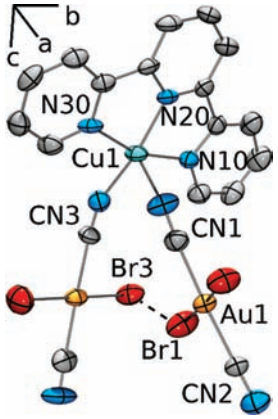

Figure 7. Molecular structure of **8** (hydrogen atoms removed for clarity). Intramolecular Br···Br contact is shown by a dashed line. CN1 represents the group containing atoms C1 and N1. Au, yellow; Br, scarlet; Cu, l; blue; C, gray; N, blue.

Table 1. Selected Bond Lengths (Å) and Angles (deg) in **8**

Bond Lengths (Å)	
Cu(1)−N(1)	2.214(10)
Cu(1)−N(3)	1.991(10)
Cu(1)−N(10)	2.032(9)
Cu(1)−N(20)	1.934(8)
Cu(1)−N(30)	2.014(8)
Br(1)−Br(3)	3.6481(19)
Bond Angles (deg)	
N(1)−Cu(1)−N(3)	88.9(4)
N(1)−Cu(1)−N(20)	106.3(4)
N(1)−Cu(1)−N(30)	93.7(4)
N(10)−Cu(1)−N(3)	97.4(4)
N(10)−Cu(1)−N(20)	80.2(3)

The Au−C and Au−Br distances of 1.982(11) and 2.4166(13) Å, respectively, are comparable to those of the free $[AuBr_2(CN)_2]^-$ anions in **1**. The Cu−NC distance of the basal $[AuBr_2(CN)_2]^-$ unit is 1.991(10) Å; the distance to the apical $[AuBr_2(CN)_2]^-$ unit of 2.214(10) Å is significantly longer, as expected.[40]

The structure also contains an intramolecular Br···Br interaction between the $[AuBr_2(CN)_2]^-$ ligands. The Br···Br distance is 3.6481(19) Å. No significant intermolecular interactions are observed.

The addition of $Ni(NO_3)_2 \cdot 6H_2O$, 2 equivalents of ethylenediamine (en), and 2 equivalents of $[^nBu_4N][AuBr_2(CN)_2]$ in MeOH yielded amber crystals of $[Ni(en)_2(AuBr_2(CN)_2)]$-$[AuBr_2(CN)_2] \cdot MeOH$ (**9**). The IR spectrum contained ν_{CN} peaks at 2209 and 2173 cm^{-1}, consistent with bound and free $[AuBr_2(CN)_2]^-$ units, respectively.

The X-ray crystal structure revealed a linear 1-D coordination polymer built up of $Ni(en)_2^{2+}$ centers bridged by $[AuBr_2(CN)_2]^-$ units. The Ni(II) centers are bound to the $[AuBr_2(CN)_2]^-$ units through N-cyano ligands (see Figure 8) with a Ni−NC distance of 2.101(8) Å.[8,40] Although the intermolecular Br−Au−Br moieties are aligned in a parallel fashion, there is little or no Br···Br interaction between chains; the closest such distance is 3.753(2) Å. However, layers of free $[AuBr_2(CN)_2]^-$ units are situated between layers of the chains and, as in **1** and **2**, these

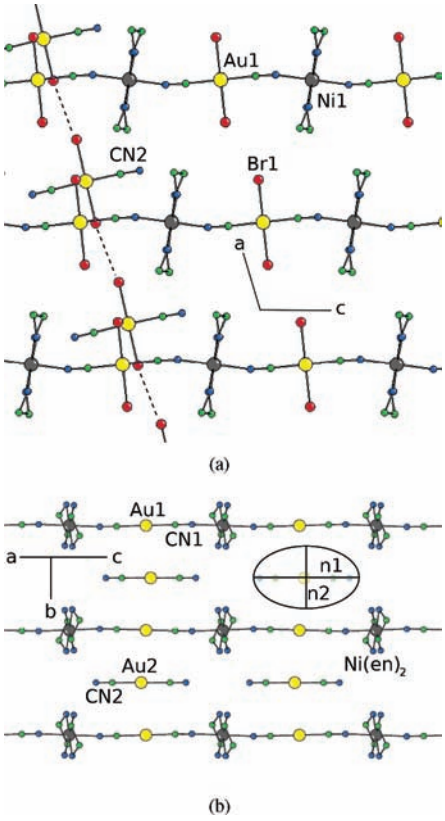

Figure 8. Structure of **9** (hydrogen atoms removed for clarity). (a) View down the *b* axis (perpendicular to the (010) plane). Only one subchain of unbound $[AuBr_2(CN)_2]^-$ units is shown. (b) View of the (100) plane. Here, the Br−Au−Br units are oriented perpendicular to the plane of view. These bromide atoms are removed for clarity. The corresponding section of the optical indicatrix representing the measured birefringence is shown. All interstitial MeOH units are removed for clarity. CN2 represents the group containing atoms C2 and N2. Au, yellow; Br, scarlet; Ni, gray; C, green; N, blue.

unbound units form additional 1-D chains via 3.583(3) Å interactions, and an Au−Br···Br angle of 171.65(10). This represents the first structurally characterized example of a coordination polymer with $[AuX_2(CN)_2]^-$ building blocks.

When viewed perpendicular to the (100) plane, as in Figure 8b, a layered structure is seen, with alternating layers of $Ni(en)_2[AuBr_2(CN)_2]^+$ coordination polymer chains and free $[AuBr_2(CN)_2]^-$ units. When viewed down the *b* axis, not only are the Br−Au−Br bonds from separate coordination polymer chains aligned in the same direction but those from the free $[AuBr_2(CN)_2]^-$ units are nearly aligned in a parallel fashion with those in the chain. This total parallel alignment of highly polarizable Au−Br bonds throughout the crystal could result in a highly birefringent material.

Birefringence Measurements. The birefringence of a material is dependent on its structure. For example, in calcite, a birefringence of $\Delta n = 0.172$ arises from the planar alignment of CO_3^{2-} anions.[31−33,54] The crystal morphology is also an important consideration, as this determines the direction down which the birefringence can be measured. In the calcite example, if viewed perpendicularly to the CO_3^{2-} planes, the birefringence will appear to be zero, whereas the value is as stated above when viewed along the planes. Thus, it is important to examine the structures of materials in order to gain insight into the origin of any birefringence. The birefringence values of both **1** and **9** were measured and are described below—both materials crystallize in a monoclinic crystal class, and are therefore biaxial; i.e., the optical indicatrix consists of three unique indices of refraction. Only one Δn value (a slice of the optical indicatrix) was measured due to crystal growth constraints.

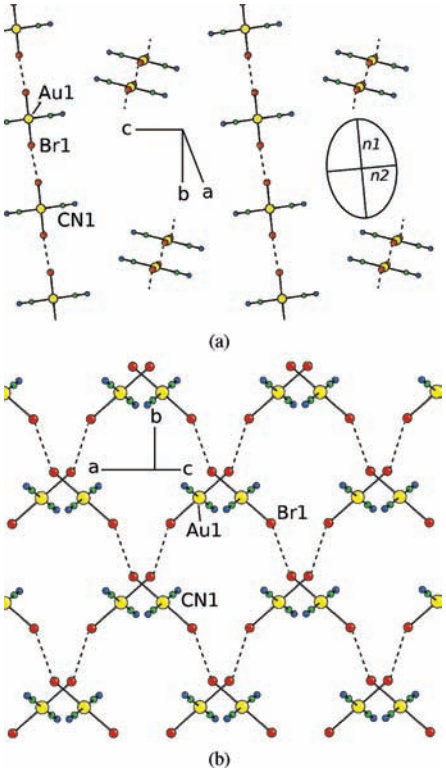

Figure 9. Superstructure of **1** ($^nBu_4N^+$ ions ommitted for clarity). (a) View of the $(1\bar{1}0)$ plane. Chains formed by Br···Br interactions are shown. Between these sets of chains are similar chains propagating approximately perpendicular to the plane of view. The corresponding section of the optical indicatrix is shown. (b) View down the (001) plane. Here, two sets of chains, formed by $[AuBr_2(CN)_2]^-$ anions connected by Br···Br interactions, can be seen propagating nearly perpendicularly to each other. This global cancellation of the polarizabilities of the Br−Au−Br bonds results in an overall nearly isotropic structure when viewed down this axis. CN1 represents the group containing atoms C1 and N1. Au, yellow; Br, scarlet; C, green; N, blue.

Birefringence of $[^nBu_4N][AuBr_2(CN)_2]$. The birefringence of **1** was determined to be $\Delta n = 0.051(4)$ in the $(1\bar{1}0)$ plane. Views of this and the (001) planes are shown in Figure 9. When viewed down the $(1\bar{1}0)$ plane, there are sets of $[AuBr_2(CN)_2]^-$ chains connected by Br···Br interactions both parallel and perpendicular to the direction of measure. The parallel Au−Br bonds are expected to contribute little to the birefringence (assuming the anisotropy of local electric fields is not large); however, the perpendicular chains show a perfect alignment of Br−Au−Br bonds in the plane of measurement, which is ideal for augmenting birefringence in theory. In fact, a significant, but not very large, birefringence value in this direction was observed. This shows that one set of Br−Au−Br bonds is slightly more than enough to offset the birefringence contribution of two sets of NC−Au−CN bonds,

(54) Bragg, W. L. *Proc. R. Soc. London, Ser. A* **1924**, *105*, 370.

which are oriented exactly perpendicular to the Br−Au−Br axis. This indicates that the polarizable Au−Br bonds could indeed significantly impact the birefringence if suitably oriented.

By changing the crystallization conditions (i.e., crystallizing from a boiling EtOH solution), poor-quality crystals could be grown with (001) as the primary face. Despite this poor crystal quality, the birefringence in this plane was determined by means of measurements of the refractive index in different directions. Using this technique, an index of refraction of $n = 1.59(3)$, independent of direction, was determined; therefore $\Delta n < 0.03$, the experimental error of this measurement. As seen in Figure 9b, a view down the *c* axis shows chains oriented nearly perpendicular to each other. The nearly isotropic arrangement with the NC−Au−CN axis down the view axis and the Br−Au−Br units globally canceling each other out would be expected to give little or no birefringence, as observed.

Birefringence of $[Ni(en)_2(AuBr_2(CN)_2)][AuBr_2(CN)_2]\cdot MeOH$. The birefringence of **9** was determined to be $\Delta n = 0.131(3)$, a significant value comparable to calcite. Crystals of **9** grow along the *a* axis, whereby the structure is viewed along the Br−Au−Br bonds (Figure 8b). As a result, the Δn value down this axis is more representative of the polarizability of the Ni−NC−Au−CN−Ni chains than of the Au−Br bonds, which are not expected to give a large contribution to Δn (again, assuming the anisotropy of the local electric fields is low in the region). Thus, although we were unable to determine the effect of the polarizable Au−Br bonds on birefringence in this case (since crystals with the desired (010) face could not be grown), it is clear that the polarizability of the cyanometallate coordination polymer chains is not negligible. In fact, it can augment or cancel out/detract from the overall birefringence depending on the relative alignment of the chain with other components. This demonstrates that it is important to also take the cyanometallate chain orientations into account when targeting enhanced birefringence.

Conclusions

The propensity of the new $[AuBr_2(CN)_2]^-$ building block to form transition-metal coordination polymers has been surveyed. In conjunction with heterocyclic amine ancillary ligands, most compounds produced contained coordinatively saturated metal cations, precluding coordination polymer formation; this indicates that the N-cyano groups of the $[AuBr_2(CN)_2]^-$ unit are quite weak Lewis bases, especially compared with the d^{10} $[Au(CN)_2]^-$,[19,55] for example. With ethylenediamine as an ancillary ligand on Ni(II), a new 1-D coordination polymer (**9**) was synthesized. Irrespective of coordination polymer formation, or lack thereof, the presence of Br···Br interactions played a large role in determining the supramolecular structure of the materials containing the $[AuBr_2(CN)_2]^-$ unit; in most cases, this resulted in the parallel alignment of highly polarizable Au−Br bonds, a potentially important factor in enhancing birefringence.

The birefringence of two materials was determined. The Δn value for **9** showed that the polarizability contribution of the NC−Au−CN bonds is quite significant. Although, due to the growth direction of the crystals, the impact of the oriented Au−Br bonds on Δn could not be determined from **9**, the Δn values for $[^nBu_4N][AuBr_2(CN)_2]$ (**1**) showed that the Br−Au−Br chains, if aligned well, can compensate for and, in fact, overcome the contribution to birefringence of the NC−Au−CN chains. This, in combination with their tendency to aggregate in an aligned fashion, suggests that Au−X bonds (and presumably other suitably oriented metal halides) are a viable tool for enhancing birefringence in coordination polymer materials.

Experimental Section

General Procedures. ***Caution!*** *Perchlorate salts are potentially explosive and are powerful oxidants. Although no difficulties have been experienced, they should be handled with care. Bromine should only be handled in a well-ventilated fumehood.*

All reactions were conducted in air. $[^nBu_4N][Au(CN)_2]\cdot 1/2H_2O$ was synthesized using literature procedures.[8] All other reagents, including 1,10-phenanthroline (phen), 2,2′;6′,2″-terpyridine (terpy), and ethylenediamine (en), were obtained from commercial sources and used as received.

IR spectra were recorded on a Thermo Nicolet Nexus 670 FT-IR spectrometer equipped with a Pike MIRacle attenuated total reflection (ATR) sampling accessory, or as KBr pellets as stated. Microanalyses (C, H, N) were performed by Frank Haftbaradaran at Simon Fraser University on a Carlo Erba EA 1110 CHN elemental analyzer.

Synthetic Procedures. **$[^nBu_4N][AuBr_2(CN)_2]$ (1).** This preparation is based on the literature procedure for $[Me_4N][AuBr_2(CN)_2]$.[47] To a 15 mL aqueous solution of $K[Au(CN)_2]$ (2.025 g; 7.03 mmol) was added 3 mL of neat Br_2, resulting in a mixture of dark brown Br_2 and a yellow solution. Excess Br_2 was removed by bubbling N_2 gas through the solution, resulting in an orange solution. To this, a 25 mL aqueous solution of $^nBu_4NBr$ (2.520 g; 7.83 mmol) was added, resulting in an immediate pale yellow precipitate of $[^nBu_4N][AuBr_2(CN)_2]$ (**1**), which was collected by vacuum filtration and allowed to air-dry overnight (4.134 g; 90% yield). IR (KBr, cm^{-1}): 2165 (w; ν_{CN}); 2976 (s), 2965 (s), 2932 (s), 2876 (s), 2862 (s), 1493 (m), 1463 (m), 1419 (w), 1379 (mw), 1155 (w), 1110 (mw), 1029 (w), 880 (m), 799 (w), 741 (m). Anal. calcd for $C_{18}H_{36}N_3AuBr_2$: C, 33.28%; H, 5.59%; N, 6.47%. Found: C, 33.20%; H, 5.62%; N, 6.23%.

Crystals suitable for X-ray analysis and birefringence measurements were grown by slow evaporation of a MeOH solution. Crystals with the (001) plane as their primary face were grown by cooling of a saturated, hot, EtOH solution and were used for refractive index measurements down the *c* axis.

$[^nBu_4N][AuI_2(CN)_2]$ (2). A 5 mL solution of $[^nBu_4N][Au(CN)_2]\cdot 1/2H_2O$ (101 mg; 0.20 mmol) was added to a 25 mL purple CH_2Cl_2 solution of I_2 (56 mg; 0.22 mmol), resulting in an orange solution. This mixture was left to evaporate to dryness, leaving dark orange flake-shaped crystals of $[^nBu_4N][AuI_2(CN)_2]$ (**2**; 144 mg; 95% yield). IR (ATR, cm^{-1}): 2165 (w; ν_{CN}); 2958 (s), 2928 (m), 2871 (m), 1485 (ms), 1453 (m), 1379 (m), 1150 (w), 1107 (mw), 1062 (mw), 1027 (mw), 880 (s), 787 (w), 738 (s). Anal. calcd for $C_{18}H_{36}N_3AuI_2$: C, 29.01%; H, 4.87%; N, 5.64%. Found: C, 29.01%; H, 4.80%; N, 5.83%.

$[Fe(phen)_3][AuBr_2(CN)_2]_2$ (3). A 10 mL MeOH solution of phen (51 mg; 0.26 mmol) was added to a 10 mL yellow MeOH solution of $Fe(ClO_4)_2\cdot xH_2O$ (30 mg; 0.12 mmol), resulting in an intense red solution. To this, a 30 mL yellow MeOH solution of $[^nBu_4N][AuBr_2(CN)_2]$ (135 mg; 0.21 mmol) was added, resulting in no visible change. The solution was partially covered and set aside. After one day, small dark red needle-shaped crystals of $[Fe(phen)_3][AuBr_2(CN)_2]_2$ (**3**) formed and were collected by vacuum filtration (89 mg; 62% yield). IR (KBr, cm^{-1}): 2169 (w; ν_{CN}); 3084 (w), 3057 (w), 1422 (s), 1219 (mw), 1204 (mw),

(55) Katz, M.; Ramnial, T.; Yu, H.; Leznoff, D. *J. Am. Chem. Soc.* **2008**, *130*, 10662.

Table 2. Crystallographic Data for Compounds **1**–**5**

	1	**2**	**3**	**4**	**5**
empirical formula	$C_{18}H_{36}N_3AuBr_2$	$C_{18}H_{36}N_3AuI_2$	$C_{40}H_{24}N_{10}Au_2Br_4Fe$	$C_{40}H_{24}N_{10}Au_2Br_4Ni$	$C_{34}H_{22}N_{10}Au_2Br_4Ni$
fw ($g \cdot mol^{-1}$)	651.28	745.28	1414.09	1416.94	1342.86
cryst syst	monoclinic	monoclinic	monoclinic	monoclinic	triclinic
space group	$C2/c$	$P2_1/n$	$P2_1/c$	$P2_1/c$	$P\bar{1}$
a (Å)	9.7350(4)	12.363(3)	11.1759(8)	11.188(2)	12.556(4)
b (Å)	12.8898(6)	17.928(4)	22.6794(15)	22.743(4)	13.072(2)
c (Å)	20.3423(10)	13.020(3)	16.5069(11)	16.691(3)	13.472(2)
α (deg)	90	90	90	90	118.012(2)
β (deg)	103.000(3)	116.446(2)	92.4240(10)	92.483(2)	97.324(3)
γ (deg)	90	90	90	90	92.434(2)
V ($Å^3$)	2487.2(2)	2582.4(10)	4180.1(5)	4243.0(13)	1922.9(8)
Z	4	4	4	4	4
T (K)	293	293	293	293	293
ρ_{calcd} ($g \cdot cm^{-3}$)	1.739	1.917	2.247	2.218	2.319
μ $(mm)^{-1}$	9.133	8.093	11.211	11.147	12.291
R, R_w $[I_0 \geq 2.50\sigma(I_0)]$[a]	0.0301, 0.0285	0.0518, 0.0671	0.0367, 0.0477	0.0413, 0.0471	0.0359, 0.0482
goodness of fit	1.0647	1.1494	1.0839	0.9800	1.0283
reflns $[I_0 \geq 2.50\sigma(I_0)]$	2352	2903	5068	4285	5723

[a] Function minimized: $\sum w(|F_o| - |F_c|)^2$, where $w^{-1} = [\sigma^2(F_o) + (nP)^2 + mP]$, with $n = 0$ and $m = 0.03$ for **1**, $n = 0.02$ and $m = 0.1$ for **2**–**4**, and $n = 0$ and $m = 0.1$ for **5**, and where $P = 1/3(F_o + 2F_c)$. $R = \sum||F_o| - |F_c||/\sum|F_o|$ and $R_w = [\sum w(|F_o| - |F_c|)^2/\sum w|F_o|^2]^{1/2}$.

1142 (mw), 1094 (mw), 841 (s), 776 (mw), 724 (s). Anal. calcd for $C_{40}H_{24}N_{10}Au_2Br_4Fe$: C, 33.98%; H, 1.71%,; N, 9.91%. Found: C, 34.28%; H, 1.76%; N, 10.02%.

[Ni(phen)$_3$][AuBr$_2$(CN)$_2$]$_2$ (4). A 5 mL MeOH solution of phen (65 mg; 0.33 mmol) was added to a 5 mL MeOH solution of $Ni(ClO_4)_2 \cdot 6H_2O$ (42 mg; 0.11 mmol), resulting in a faint pink solution. To this, a 30 mL yellow MeOH solution of [^{n}Bu$_4$N][AuBr$_2$(CN)$_2$] (133 mg; 0.20 mmol) was added, resulting in no visible change. The solution was partially covered and set aside. After one day, amber needle-shaped crystals of [Ni(phen)$_3$][AuBr$_2$(CN)$_2$]$_2$ (**4**) formed and were collected by vacuum filtration (103 mg; 71% yield). IR (KBr, cm^{-1}): 2168 (w; ν_{CN}); 3057 (w), 1626 (mw), 1589 (mw), 1516 (m), 1422 (s), 1339 (mw), 1221 (mw), 1140 (m), 1103 (m), 869 (mw), 843 (s), 776 (w), 724 (s), 643 (mw). Anal. calcd for $C_{40}H_{24}N_{10}Au_2Br_4Ni$: C, 33.91%; H, 1.71%; N, 9.89%. Found: C, 34.18%; H, 1.74%; N, 10.05%.

[Ni(terpy)$_2$][AuBr$_2$(CN)$_2$]$_2$ (5). A 10 mL MeOH solution of terpy (37 mg; 0.16 mmol) was added to a 10 mL MeOH solution of $Ni(ClO_4)_2 \cdot 6H_2O$ (40 mg; 0.11 mmol), resulting in an amber solution. To this was added a 30 mL yellow MeOH solution of [^{n}Bu$_4$N][AuBr$_2$(CN)$_2$] (132 mg; 0.20 mmol), resulting in no visible change. The solution was partially covered and set aside. After a few days, red block-shaped crystals of [Ni(terpy)$_2$][AuBr$_2$(CN)$_2$]$_2$ (**5**) formed and were collected by vacuum filtration (38 mg; 28% yield). IR (KBr, cm^{-1}): 2168 (w; ν_{CN}); 3077 (w), 1599 (s), 1578 (m), 1470 (ms), 1450 (s), 1419 (w), 1320 (m), 1246 (mw), 1188 (w), 1161 (mw), 1093 (mw), 1014 (m), 781 (s), 767 (s), 650 (m). Anal. calcd for $C_{34}H_{22}N_{10}Au_2Br_4Ni$: C, 30.41%; H, 1.65%; N, 10.43%. Found: C, 30.79%; H, 1.66%; N, 10.71%.

[Fe(terpy)$_2$][AuBr$_2$(CN)$_2$][ClO$_4$] (6). A 10 mL MeOH solution of terpy (30 mg; 0.13 mmol) was added to a 5 mL yellow MeOH solution of $Fe(ClO_4)_2 \cdot xH_2O$ (31 mg; 0.12 mmol), resulting in an intense purple solution. To this was added a 25 mL yellow MeOH solution of [^{n}Bu$_4$N][AuBr$_2$(CN)$_2$] (133 mg; 0.20 mmol), resulting in no visible change. The solution was partially covered and set aside. After one day, small dark purple plate-shaped crystals of [Fe(terpy)$_2$][AuBr$_2$(CN)$_2$][ClO$_4$] (**6**) formed and were collected by vacuum filtration (19 mg; 18% yield). IR (KBr, cm^{-1}): 2168 (w; ν_{CN}); 3074 (w), 1604 (m), 1450 (s), 1369 (mw), 1285 (mw), 1242 (w), 1088 (br; ν_{ClO4}), 768 (s), 623 (m). Anal. calcd for $C_{32}H_{22}N_8O_4AuBr_2ClFe$: C, 37.29%; H, 2.15%; N, 10.87%. Found: C, 37.33%; H, 2.15%; N, 11.08%.

[Cu(phen)$_2$(NO$_3$)][AuBr$_2$(CN)$_2$] (7). A 5 mL MeCN solution of phen (44 mg; 0.26 mmol) was added to a 5 mL light blue MeCN solution of $Cu(NO_3)_2 \cdot 6H_2O$ (26 mg; 0.11 mmol), resulting in a more intense blue solution. To this was added a 5 mL yellow MeCN solution of [^{n}Bu$_4$N][AuBr$_2$(CN)$_2$] (135 mg; 0.21 mmol), resulting in a green solution. After a few minutes, green plate-shaped crystals of [Cu(phen)$_2$(NO$_3$)][AuBr$_2$(CN)$_2$] (**7**) formed and were collected by vacuum filtration (86 mg; 99% yield). IR (ATR, cm^{-1}): 2165 (w; ν_{CN}); 3060 (w), 1584 (mw), 1519 (m), 1445 (m, ν_{NO_3}), 1426 (s), 1293 (s, ν_{NO_3}), 1256 (w), 1223 (mw), 1143 (mw), 1106 (mw), 1034 (m, ν_{NO_3}), 849 (s), 781 (m), 721 (s). Anal. calcd for $C_{26}H_{16}N_7O_3AuBr_2Cu$: C, 34.90%; H, 1.80%; N, 10.96%. Found: C, 34.86%; H, 1.80%; N, 10.91%.

Cu(terpy)[AuBr$_2$(CN)$_2$]$_2$ (8). A 10 mL MeOH solution of terpy (38 mg; 0.16 mmol) was added to a 10 mL light blue MeOH solution of $Cu(ClO_4)_2 \cdot 6H_2O$ (45 mg; 0.12 mmol), resulting in a more intense blue solution. To this, a 20 mL yellow MeOH solution of [^{n}Bu$_4$N][AuBr$_2$(CN)$_2$] (135 mg; 0.21 mmol) was added, resulting in a green solution. After a few minutes, green needle-shaped crystals of Cu(terpy)[AuBr$_2$(CN)$_2$]$_2$ (**8**) formed and were collected by vacuum filtration (80 mg; 70% yield). IR (KBr, cm^{-1}): 2222 (w; ν_{CN}), 2206 (w; ν_{CN}), 2177 (w; ν_{CN}); 3076 (w), 1597 (ms), 1578 (m), 1478 (s), 1446 (s), 1327 (mw), 1252 (mw), 1164 (m), 1122 (s), 1090 (m), 1025 (ms), 779 (vs), 731 (m), 752 (m). Anal. calcd for $C_{19}H_{11}N_9Au_2Br_4Cu$: C, 20.48%; H, 1.00%; N, 8.80%. Found: C, 20.90%; H, 1.05%; N, 8.69%.

[Ni(en)$_2$(AuBr$_2$(CN)$_2$)][AuBr$_2$(CN)$_2$]·MeOH (9). A 2 mL MeOH solution of a 0.1 M stock solution of en (0.20 mmol) was added to a 5 mL green MeOH solution of $Ni(NO_3)_2 \cdot 6H_2O$ (30 mg; 0.10 mmol), resulting in a purple solution. To this was added a 10 mL yellow MeOH solution of [^{n}Bu$_4$N][AuBr$_2$(CN)$_2$] (129 mg; 0.20 mmol), resulting in a yellow solution. The solution was partially covered and set aside. After two days, amber plate-shaped crystals of [Ni(en)$_2$(AuBr$_2$(CN)$_2$)][AuBr$_2$(CN)$_2$]·MeOH (**9**) formed and were collected by vacuum filtration (29 mg; 29% yield). IR (KBr, cm^{-1}): 2209 (w; ν_{CN}), 2173 (w, ν_{CN}); 3483 (br; ν_{OH}), 3332 (vs), 3288 (s), 3175 (w), 2957 (w), 2889 (w), 2839 (w), 1593 (m), 1454 (w), 1363 (w), 1280 (w), 1102 (mw), 1022 (vs), 969 (m), 674 (m), 521 (m). Anal. calcd for $C_9H_{12}N_8Au_2Br_4NiO$: C, 10.51%; H, 1.96%; N, 10.89%. Found: C, 10.65%; H, 1.91%; N, 10.99%.

Single Crystal X-Ray Diffraction Structure Determinations. All crystalline samples were mounted on glass fibers using epoxy adhesive, and the data were collected at room temperature. Additional crystallographic information can be found in Tables 2 and 3.

Table 3. Crystallographic Data for Compounds **6**–**9**

	6	**7**	**8**	**9**
empirical formula	$C_{32}H_{22}N_8O_4AuBr_2ClFe$	$C_{26}H_{16}N_7O_3AuBr_2Cu$	$C_{19}H_{11}N_9Au_2Br_4Cu$	$C_9H_{12}N_8Au_2Br_4NiO$
fw ($g \cdot mol^{-1}$)	1030.65	894.78	1142.45	1020.49
cryst syst	orthorhombic	triclinic	monoclinic	monoclinic
space group	$P2_12_12_1$	$P\bar{1}$	$P2_1/c$	$P2_1/m$
a (Å)	8.8874(15)	10.4717(3)	7.6901(3)	8.4178(3)
b (Å)	9.1081(16)	11.2175(4)	16.0919(6)	14.1538(6)
c (Å)	42.151(7)	13.0264(5)	20.6901(7)	10.3633(4)
α (deg)	90	114.956(2)	90	90
β (deg)	90	92.120(2)	94.091(2)	106.587(2)
γ (deg)	90	93.991(2)	90	90
V ($Å^3$)	3412.0(10)	1380.20(9)	2553.84(16)	1183.34(8)
Z	4	2	4	2
T (K)	293	293	293	293
ρ_{calcd} ($g \cdot cm^{-3}$)	2.006	2.153	2.898	2.875
μ (mm^{-1})	7.191	9.017	18.567	19.922
R, R_w [$I_0 \geq 2.50\sigma(I_0)$][a]	0.0420, 0.0431	0.0372, 0.0411	0.0459, 0.0528	0.0451, 0.0660
goodness of fit	1.1758	1.0254	1.0402	1.1586
reflns [$I_0 \geq 2.50\sigma(I_0)$]	5444	4108	4456	2826

[a] Function minimized: $\sum w(|F_o| - |F_c|)^2$, where $w^{-1} = [\sigma^2(F_o) + (nP)^2 + mP]$ with $n = 0.020$ and $m = 0$ for **6**, $n = 0.01$ and $m = 0.03$ for **7**, and $n = 0.02$ and $m = 0.1$ for **8** and **9**, and where $P = 1/3(F_o + 2F_c)$. $R = \sum||F_o| - |F_c||/\sum|F_o|$ and $R_w = [\sum w(|F_o| - |F_c|)^2/\sum w|F_o|^2]^{1/2}$.

All diffraction data were processed with the Bruker Apex II software suite. The structures were solved with Sir92. Subsequent refinements were performed in Crystals.[56]

The C and N atoms of **3** were refined isotropically due to limitations of the data. In **5**, the distance between atoms C3 and N3 was restrained to the distances of the other cyano distances in the asymmetric unit. Compound **9** contains a disordered free MeOH unit. The disorder was refined, but isotropically.

Diagrams were made using ORTEP-3,[57] POV-RAY,[58] and Cameron.[59]

Birefringence. The optical retardation values were measured on plate-shaped crystals of **1** and **9** by means of polarized-light microscopy using an Olympus BX60 microscope, with a tilted Berek compensator at $\lambda = 546$ nm at room temperature. The birefringence was calculated by dividing the measured retardation by the crystal thickness. The thickness was measured on a Strata DB235 FESEM/FIB dual beam scanning electron microscope. The orientation of the slice of the optical indicatrix in the viewing plane was determined using single-crystal X-ray diffraction techniques.

The birefringence of **1** in the (001) plane was determined using a Metricon Model 2010/M Prism Coupler at $\lambda = 1552$ nm. Crystals of **1** grown with this plane as the primary face were not of sufficient quality to use optical microscopy to determine Δn. Refractive index measurements were made while incrementing the angle of the crystal with respect to electrical polarization of the laser beam. The variations of the index of refraction were below the experimental error ($\delta n = \pm 0.03$) associated with the measurements of these poor crystals.

Acknowledgment. The authors thank NSERC of Canada and the World Gold Council GROW program for financial support, and the Province of British Columbia for a Pacific Century Graduate Scholarship (J.S.O.).

Supporting Information Available: Single-crystal X-ray crystallographic data in CIF format for all compounds. This material is available free of charge via the Internet at http://pubs.acs.org.

(56) Betteridge, P. W.; Carruthers, J. R.; Cooper, R. I.; Prout, K.; Watkin, D. J. *J. Appl. Crystallogr.* **2003**, *36*, 1487.
(57) Farrugia, L. J. *J. Appl. Crystallogr.* **1997**, *30*, 565.
(58) Fen, T. D.; Ringe, D.; Petsko, G. A. *J. Appl. Crystallogr.* **2003**, *36*, 944.
(59) Watkin, D. J.; Prout, C. K.; Pearce, L. J. *Cameron*; Crystallography Laboratory, University of Oxford: Oxford, U. K., 1996.